Materials Research Express

CrossMark

OPEN ACCESS

RECEIVED
8 July 2021

REVISED
12 August 2021

ACCEPTED FOR PUBLICATION
18 August 2021

PUBLISHED
27 August 2021

PAPER

Influence of the carburization time on the structural and mechanical properties of XC20 steel

Saoudi Abdenour[1], Aissani Linda[2,3], Chahaoui Oualid[1,4], Bestandji Ali[5], Louafi Mohammed Salah[1], Djebaili Hamid[1] and Chinesta Francisco[6]

[1] Mechanical Engineering Department Abbes Laghrour-Khenchela University PO Box 1252, Khenchela 40004, Algeria
[2] Laboratory of Active Components and Materials Larbi Ben M'Hidi University, Oum El Bouaghi, Algeria
[3] Mater Science Department, Abbes Laghrour-Khenchela University PO Box 1252, Khenchela 40004, Algeria
[4] Engineering and Advanced Materials Science Laboratory (ISMA), Abbes Laghrour-Khenchela University, PO Box 1252, 40004, Algeria
[5] Laboratoire métallographie, ETRAG, N20 B.P 74 Oued Hamimime, El Khroub 25100, Algeria
[6] PIMM Lab & ESI Chair, Arts et Metiers Institute of Technology 151 Boulevard de l'Hôpital, 73013 Paris, France

E-mail: saoudiabdenour@gmail.com

Keywords: XC20 steel, carburization, hardening, cementite, impact, precipitation, diffusion

Abstract

This study focuses on the effect of carburization time on the structural and mechanical properties of low carbon XC20 mild steel (C. Wt.% <0.25). The XC20 steel was carburized with activated carbon with a carbon potential $Cp_1 = 1.1\%$, at 910 °C at different carburization times of 2, 4 and 6 h. The results obtained show that XC20 steel (non-carburized) has a ferrite-pearlitic structure with a hardness and a Young's modulus of the order of (150 HV, 26 KN/mm^2). After carburization, the structure of the carburized layer is transformed in martensite (Fe γ) in which cementite (Fe_3C) is imbricated. The depth of the carburized layer and the amount of carbon on the surface gradually increase with increasing carburization time. In addition, the carburized XC20 steel becomes hard and brittle where the hardness and Young's modulus have been increased for a high holding time until reaching maximum values (845 HV, 48 KN mm^{-2}) after 6 h of carburization . However, the toughness of XC20 steel has been reduced from 163 to 40 J cm^{-2}.

1. Introduction

Currently, steels are one of the most widely used materials in various industrial activities intended for the manufacture of piston pins, camshafts, levers, pump shafts, …because they are readily available, workable and weldable [1]. However mild steels with a low carbon content have less important chemical-physical and mechanical properties. For industrial applications, the middle steels have been considered a ferrite material due to its low carbon and used for automotive clutch parts, chain parts, automotive seat belt parts, springs and washers. However, the mechanical properties such as harness, toughness and resistance to stress are very poor as compared with other based carbon steels [2].

The surface layer is the area of a component that is the most exposed and stressed to chemical attack, friction and external forces. Generally, the enhanced mechanical properties superficial of steels can be achieved by changing the microstructure and chemical composition. This is typically controlled by the applied of different thermal or thermochemical treatments [3]. The usefulness of applying heat treatments to carbon steels (C% <0.25) remains limited, because this type of treatment does not improve sufficiently the surface's properties (hardness, resistance to wear and impact, fatigue, ...) to meet the severe requirements of contacting and moving parts [4–6]. Among them, carburization is one of the most effective thermochemical treatments, which aims at superficially enriching the surface with carbon in the atomic state (between 0.7 and 0.9 Wt. %) by diffusion in the austenitic phase (870 to 980 °C depending on the process) followed by quenching and eventual tempering in order to improve the surface's properties according to a decreasing gradient over a very limited depth without reaching the core [7–15]. Other hand, the presence of carbon would confine the grain refinement the steel surface, which inhibits the mobility of plastic deformation during solid-solid interactions [8, 11]. The resulting

Table 1. Chemical composition of experimental XC20 steel (Wt. %).

Component	C	Fe	Si	Mn	P	S	Cr	Ni	Cu
Wt. %	0,23	Bal.	0,27	0,45	0,018	0,014	0,057	0,040	0,096

mixture phases combine the properties of cementite (hardness) and austenite (ductility). Recently, researchers are interesting to develop steel layer surface on forming hard phases embedded more carbon with iron by carburization [6, 7]. Generally, the thermochemical treatments are based on three main phases [16–23]:

(1) A source of a diffusing element: a process whose seat is the external environment by ensuring the release of the diffusing element (carbon, nitrogen, boron...) in the atomic state.

(2) Absorption: contact of the diffusing element atoms with the surface layer of the treated part by forming chemical bonds with the iron atoms in the presence of alloying elements such as: manganese, chromium, nickel, molybdenum, boron.

(3) Diffusion: a process of penetration of the diffusing element from the saturated surface layer towards the core to a limited depth.

The hard carburized surfaces obtained after carburization treatment have an excellent harness and a high wear resistance many times better than mild steels by lubricating effect of carbon. Other hind, the iron carbides having several interesting properties become very attractive candidates for protective coatings in industrial metal cutting tools [24]. Amorphous carbon can act not only as a reactant in the formation of carbides but also as a susceptor and secondary heat source sustaining the high temperatures required for processes such as reduction and carburization [25, 26].

Adams S M *et al* [27] showed that the morphology and properties of mild steel were related to the time and temperature of carburization. Oyetunji A *et al* [28] reported that the carbon content in the steel carburized using powdered palm kernel shell and animal bone increases as temperatures increased from 800 °C to 1100 °C. Also, Eunji Y H J *et al* [29] studied the influence of carbide formation on the mechanical and tribological properties of carburized steels and found that the fine carbides increased the resistance against crack propagation and improved the mechanical properties.

However, only limited reports on in steel carburization are available; these are either discussing the microstructure and mechanical properties with different carbon content without comprehensive information on the structure transformation due to the complexity of controlling parameters in carburization [11].

In order to strengthen the steel surface for severe external applications operating at high temperature, it is required to develop the mechanical properties of XC20 steel such operating condition.

The present study aimed to study the effect of the carburization time on the mechanical properties and toughness of XC20 steels. Therefore, the structure and morphology as well as hardness of the thermochemical treated XC20 steels were thoroughly presented.

2. Experimental materials and procedures

Our study is consecrated to the carburization of XC20 mild steel, containing <0.25 wt.% of C, which belongs to the class of non-alloy steels of construction. The chemical analysis XC20 mild steel obtained by spark spectrometry (spark OES) is listed in table 1, which is generally balanced to give it a modest mechanical property.

XC20 steel samples (C_1, C_2, C_3 and C_4) with the size of 10 $\pm$ 0.1 mm in diameter and 55 $\pm$ 0.1 mm in length, they were elaborated by chip removal for Charpy U test and the dimensions are shown in figure 1.

Carburizing of the specimens was carried out in a SOLO Swiss 302-40/250 type. Sample C_1 is left untreated (raw), to compare the mechanical properties of XC20 steel before and after carburization. The samples C_2, C_3 and C_4 are carburized by varying the carburization time, the carburizing process conditions and heat treatment cycle are shown in figure 2:

1. A constant flow of methanol ($CH_3OH = 4 \times 10^{-3}\ m^3\,h^{-1}$) for the samples ($C_2$, C_3 and C_4).

2. Heating the samples (C_2, C_3 and C_4) to the austenitic phase ($T_1 = 910$ °C).

3. A carburization process at a temperature $T_1 = 910$ °C by varying the holding time, C_2 (2 h), C_3 (4 h), C_4 (6 h) at the potential constant carbon $Cp_1 = 1.1$ %.

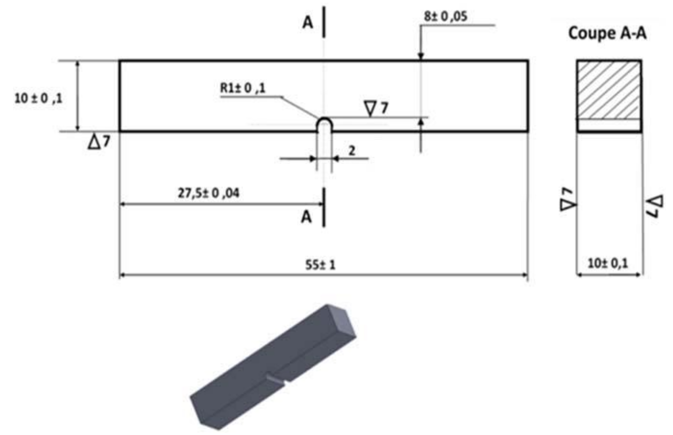

Figure 1. Dimensions of the standard Charpy U impact test samples.

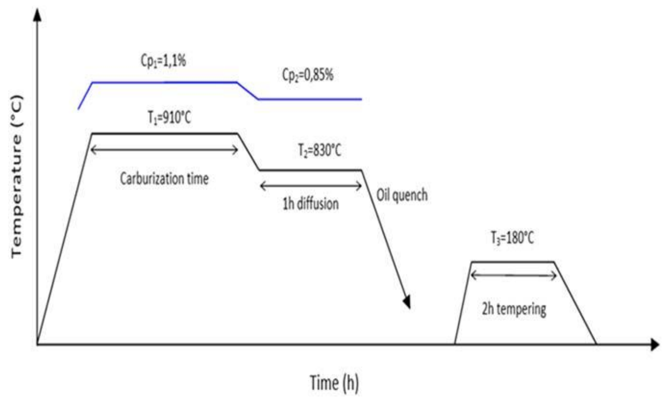

Figure 2. Diagram of the carburization treatment cycle.

4. A carbon diffusion phase at a temperature $T_2 = 830\ ^{\circ}C$ for a period of one hour for the samples (C_2, C_3 and C_4) with $Cp_2 = 0.85\ \%$.

5. An oil quench from the temperature $T_2 = 830\ ^{\circ}C$, followed by a tempering treatment at $T_3 = 180\ ^{\circ}C$ for 2 h to cause the diffusion of carbon atoms so that the XC20 steel returns to a state close to balanced (figure 2).

2.1. Characterization methods

The microstructure of the carburized samples after polishing, and etching in a 4% Nital solution, was observed on an optical inverted microscope Leica DMi8 (Germany). The Vickers hardness distribution from the carburized samples was obtained by using Zwick Roell ZHV10-A (Germany) type with a load of 500 gf for a holding time of 10 s at 20 °C. The average value of Vickers hardness was reported for three readings. The chemical composition of the samples was investigated by PECTROMAXx arc/spark OES (SPECTRO, Germany). Using the samples as shown in figure 1, Charpy tests at room temperature (20 °C) were performed on the machine of charpy Hoytom 300 J $A^{-1}D^{-2}$ type (Spain). For each test, three samples were tested and the toughness results were averaged. After charpy tests, the fracture samples were observed by a Digital camera.

3. Results and discussions

3.1. Microstructure and phase analysis

Figure 3 shows the evolution of carbon content in the surface layer of XC20 steel before and after different carburization times measured by PECTROMAX analyse. Before carburization, the surface layer shows a low carbon content of about $C = (0.23 \pm 0.01)$ Wt. %, which is corresponding to the carbon amount of XC20

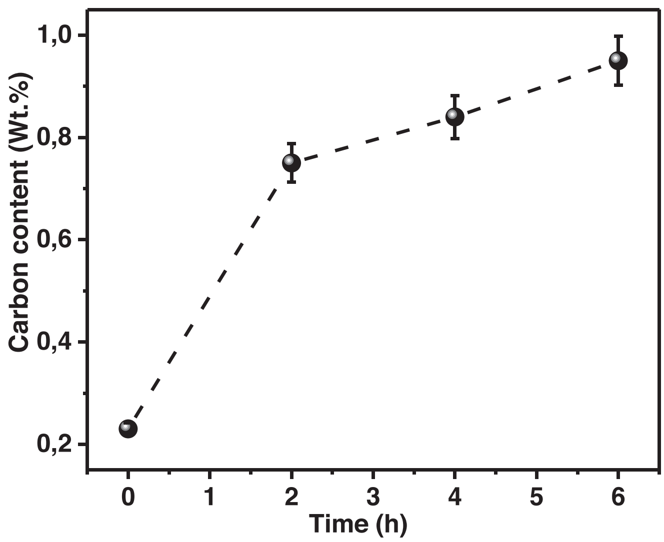

Figure 3. Evolution of the carbon content in the surface layer of XC20 steel before and after different time of carburization.

(table 1). It is obvious that carbon content in the surface layer of XC 20 samples gradually increased after carburization at (0.75 ± 0.03) Wt. %, (C_2), (0.84 ± 0.04) Wt. % (C_3) and then (0.95 ± 0.04) Wt. % (C_4) with increasing the carburization time from 2, 4 and 6 h, respectively (figure 3). It can be attributed that the diffusion of C by increasing both the rate of absorption and the carburization time that favorite the reaction with the iron of the XC20 to form new based carbon phase. Thibaux P *et al* [30] showed a similar increase in the C content in surface layer of Fe-C-Mn steels as a function of increasing of carburization time.

In order to demonstrate the influence of carburization time on the surface layer of XC20 samples and confirm consequently the difusion mechanism of carbon, different observations and measurements of thickness were performed by using an optical micropscope.

According to the obtained microstructures before carburization treatment, sample C_1 has a homogeneous structure with uniform grains of ferrite and lamellar pearlite at the core and at the edge (see figures 4(b) and (c)) [31].

After carburization, it can observed that the core of the samples C_2, C_3 and C_4 are changed from (ferrite + pearlite) to a mixture of (bainite and retained austenite, which is not transformed during quenching) (see figures 5(b), 6(b) and 7(b)) [32, 33]. However, the structure of the carburized surface layer showed the formation of the martensitic in mixture with cementite (Fe_3C, iron carbides) (see figures 5(c), 6(c) and 7(c)) [34–36]. It is also clearly observed that with increasing the carburization time, the quantity of retained austenite decreases and the contents of carbides and martensite gradually increased which would lead to the diffusion of more carbon and promotes the formation of cementite. Moreover, it was observed that the thickness of the carburizedsurface layer increased during the carburisazation treatment ($dC_2 = 840.4\ \mu m$) at 2h (figure 5(a), ($dC_3 = 1056.99\ \mu m$) at 4h (figure 6(a) and reached ($dC_4 = 1089.22\ \mu m$) at 6h (figure 7(a)). This observation was also confirmed by Rabah B *et al* [37] during the carburization of (18NC4 and 22MC4) steels.

3.2. Micro-hardness profile and measurement of carburized layer depth

Figure 8 shows the obtained microhardness profiles for XC20 steel before and after different carburization time. Before carburization, the curves of both micro-hardness and young modulus show the same tendency. For untreated XC20 sample (C_1), the hardness has the same value of about is 150 HV in the edge and the core. After carburization, the hardness profile of samples C_2, C_3 and C_4 shows three distinct zones. First, the carburized layer that has the highest surface hardness of about (757 ± 10) HV (2h), (824 ± 11) HV (4h) and (845 ± 11) HV (6 h). The high values of the hardness in the carburized layer are obtained by the quenching effect after the diffusion of an important amount of carbon in the austenitic phase and subsequently, the austenite to martensite transformation and the formation of the hard cementite (Fe_3C). Other hind, the depth of the carburized layer was calculated by an indirect microhardness measurement method following ISO 18203: 2016 at 550 HV. The values of the carburized layers gradually increased with increasing the carburization time from (dC_2, dC_3 and dC_4) are respectively equal to 825.4 μm, 1027.3 μm and 1100.5 μm, which are closed to that obtained by the optical microscope observations (figures 5, 6 and 7). The second zone presents the region of diffusion of the carbon through the XC20 steel where the hardness values are slightly decreased by decreasing the amount of carbon as a consequence of a weak austenite to martensite transformation because the cooling is slow (heat

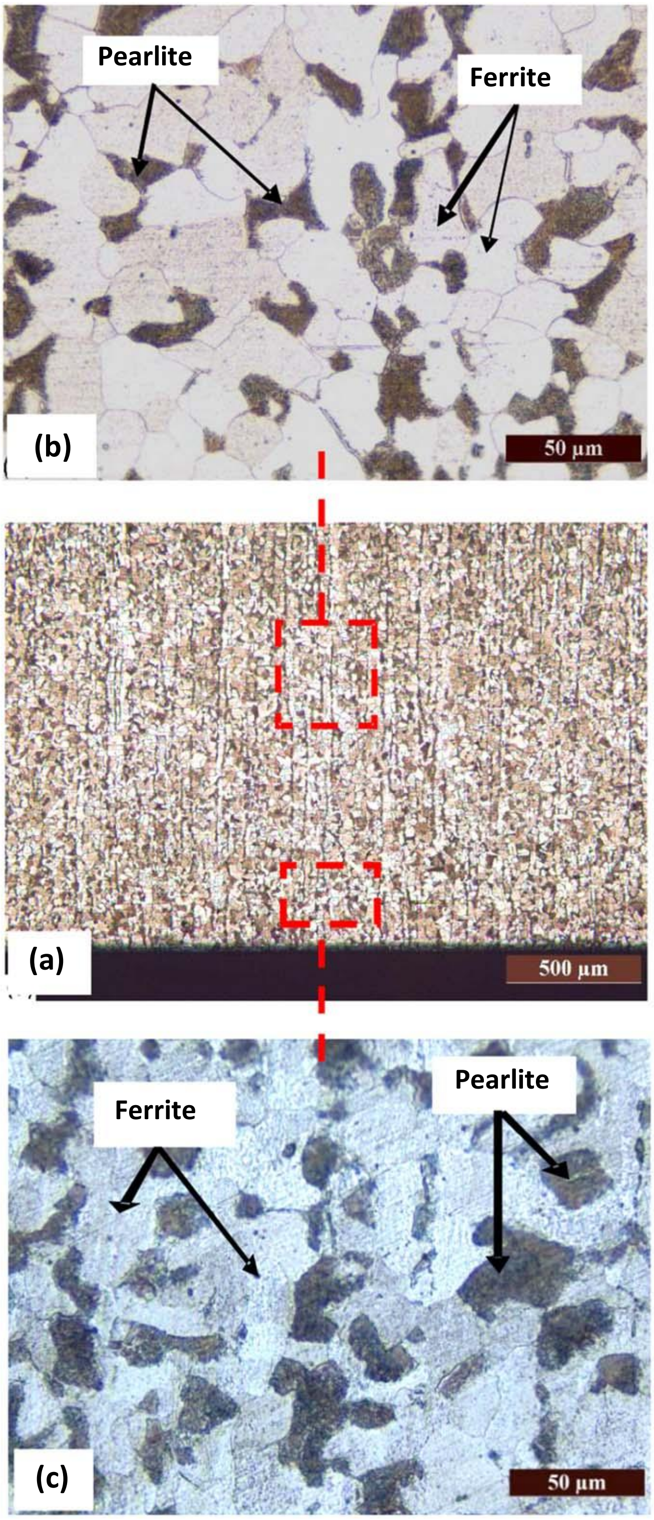

Figure 4. (a) Microstructure of XC20 sample (C_1): (b) the core, (c) the edge.

transfer by conduction). The third zone presents a low microhardness value of about (230 ± 8) HV corresponding to the core of the XC20 steel because the carburizing effect remains superficial and does not reach the core.

3.3. Toughness

The manufacturing of metal parts from mild steels must be resistant to multiple impacts. In this alternative and to test the quantity of consumed energy of XC20 steel before and after carburization treatment, 04 standardized samples (C_1, C_2, C_3 and C_4) (ASTM E23-96) were selected and characterized by an impact test of Charpy U at a

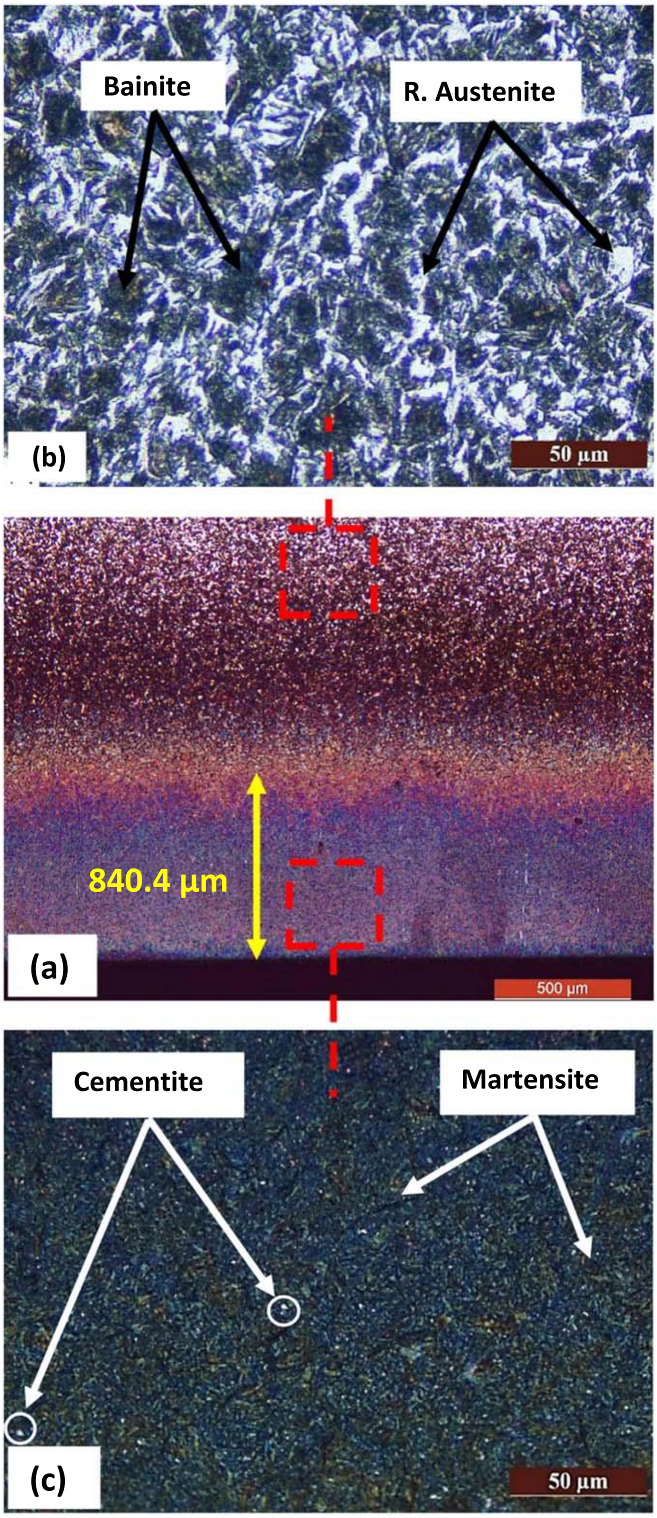

Figure 5. (a) Microstructure of XC20 sample (C_2) after 2h of carburization in the: (b) the core, (c) the edge.

standard temperature of 20 °C. Figure 9 shows the development of the toughness of XC20 steel before and after carburization. Before carburization, the C_1 specimen has the highest toughness value of about 163 J cm^{-2}. The optical images after Charpy test presents a partial fracture with a rough top view section (figure 10a), which explain a ductile feature of XC20 steel (non-carburized) containing a soft ferrite with a small amount of carbon C = 0.23 wt.% (a mild steel) [26]. After carburization, the tenacity gradually decreases as a function of the increase of the carburization time down to 58 J cm^{-2} (2h), 44 J cm^{-2} (4h) and 40 J cm^{-2} for 6 h of holding. The optical images present a total vertical brittle with a sooth top view section (figure 10, b, c and d), due to a fragile feature of the samples after the diffusion of carbon. This is due to the the increase of the depth of the carburized

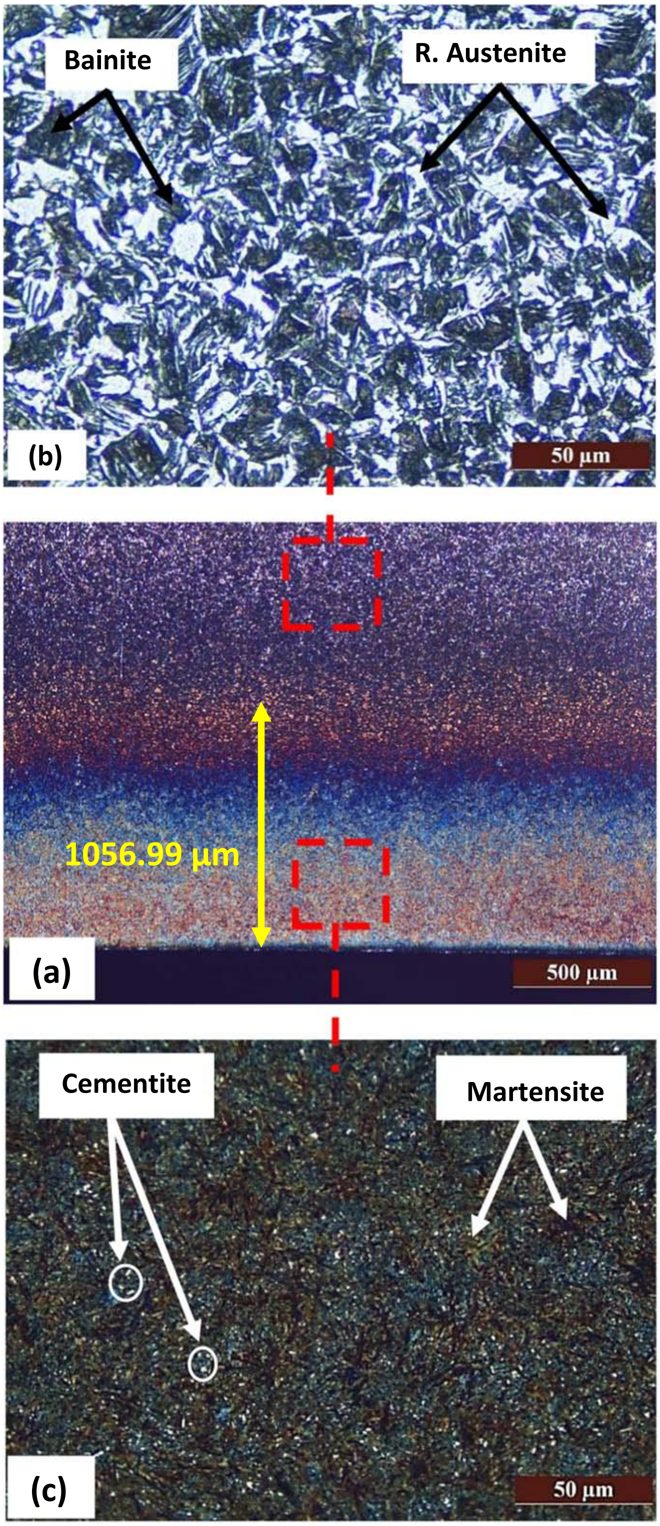

Figure 6. (a) Microstructure of XC20 sample (C_3) after 4h of carburization in the: (b) the core, (c) the edge.

surface layer the formation of solid solution strengthening phases (formation of hard martensite and cementite phases) [26] which provides a large amount of multiple crack initiation sites along the interface of hard and brittle cementite (Fe_3C). The amount of cementite is proportional to the amount of carbon diffused on the surface of the XC20 steel. The same result was obtained by Hesham E, which explained that by the high hardness [38].

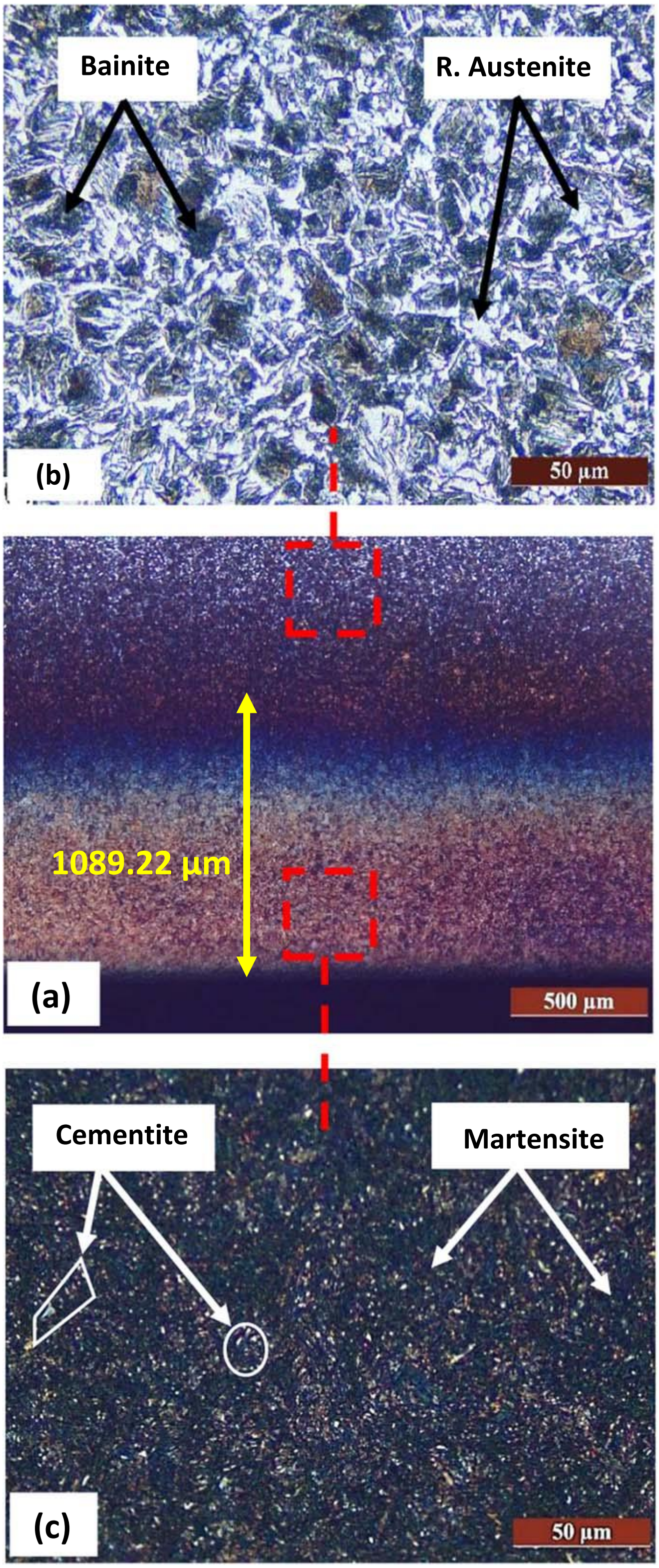

Figure 7. (a) Microstructure of XC20 sample (C_4) after 6h of carburization in the: (b) the core, (c) the edge.

4. Conclusions

In this paper, we investigated the structure, hardness, and toughness of XC20 steels before and after carburization treatment. The following conclusions can be drawn.

(1) The quantity of diffused carbon on the surface of XC20 steel and the depth of the carburized layer are proportional to the carburization time.

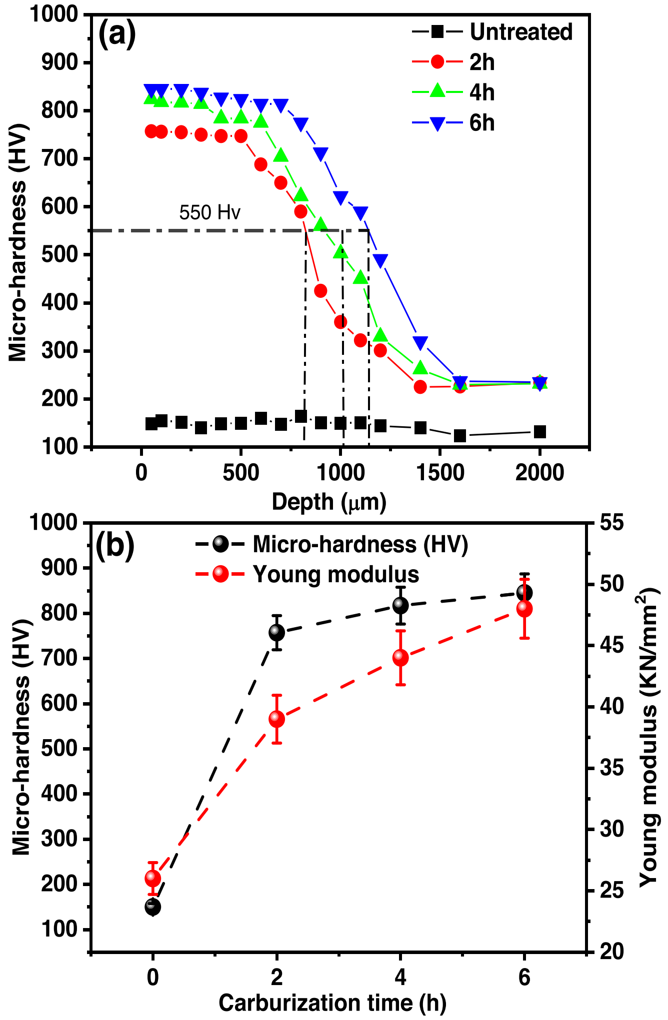

Figure 8. (a) The microhardness as a function of the penetration depth, (b) hardness and young modulus of XC 20 steel for different time of carburization.

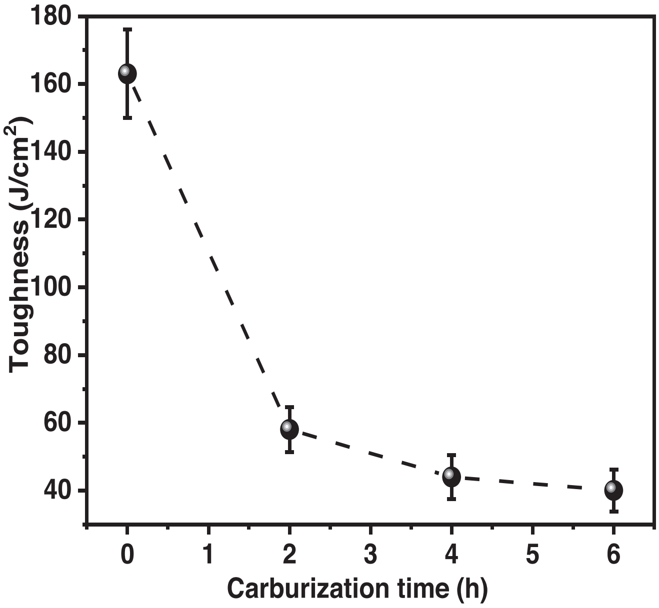

Figure 9. The effect of carburization time on the toughness of XC20 steel.

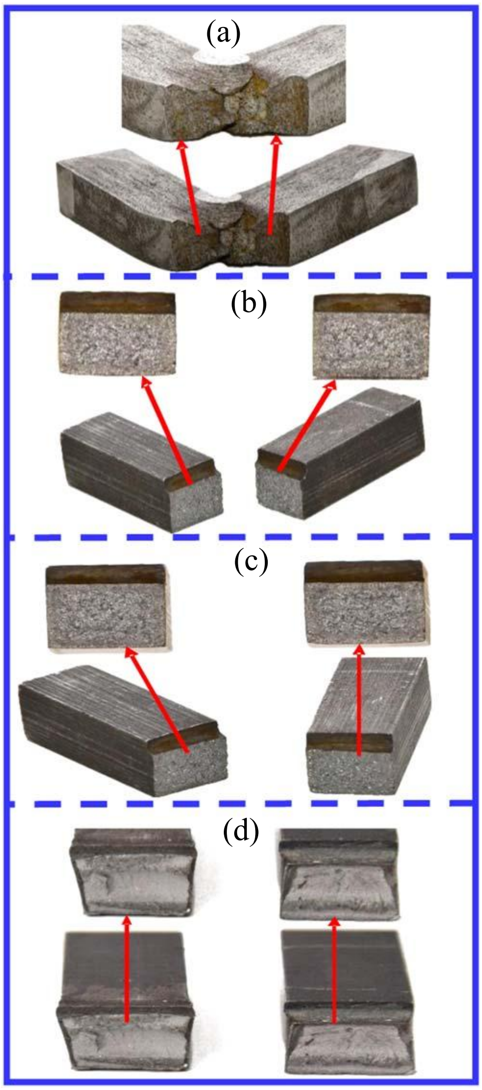

Figure 10. The optical images of XC20 steels after chapy U test: (a) C_1 : (b) C_2, (c) C_3, and (d) C_4.

The structure of the surface layer transformed from a ferrito-pearlitic structure to a (martensitic + cementite (Fe_3C)) structure after carburization.

(2) The mechanical properties of XC20 steel samples are greatly improved by the diffusion of carbon due to solid solution strengthening and the formation of hard phases. The XC20 samples carburized at 6 h containing 0.95 wt. % of carbon shows the best hardness, a highest Young modulus and lowest thogness, which is simultaneously obtained hard and resistante to deformation by the formation of the hard cementite phase at the surface.

(3) The hardness and Young modulus values of the carburized XC20 steel decrease from the carburized surface layer to the midl core. Which is the result of the association between the hard and brittle surface layer and the soft and ductile core.

(4) The carburizing treatment is widely recommended for mild XC20 for improving its mechanical properties for sever applications, significantly deteriorates, shock resistance and sometimes makes it unsuitable for other applications.

Data availability statement

The data that support the findings of this study are available upon reasonable request from the authors.

ORCID iDs

Saoudi Abdenour https://orcid.org/0000-0002-9845-0290
Chinesta Francisco https://orcid.org/0000-0002-6272-3429

References

[1] Ngafwan, Agus D A, Wibi P and Purnomo 2021 The influence of carbon particle size in the carburizing process of ST-40 steel to the surface hardness *J. Phys. Conf. Ser.* **1858** 012026
[2] Raden D R, Andra A and Rochim S 2017 The effect of thermo-mechanical treatment of substrate preparation and carburizing temperature on the morphology and hardness of carburizing on low carbon steel iop iop conf. series *Materials Science and Engineering* **214** 012025
[3] Geoffrey P 1999 Carburizing: microstructures and properties ASM International *Materials Park OH* ***978-0-87170-666-9***
[4] Mohrbacher H 2016 Metallurgical concepts for optimized processing and properties of carburizing steel *Advances in Manufacturing* **4** 105–14
[5] Wei L, Tatsuo S, Masami W and Singo M 2013 Influence of microstructure and surface defect on very high cycle fatigue properties of clean spring steel *Int. J. Fatigue* **60** 48–56
[6] Binzhou L, Changsheng L, Zhenxing L and Jingbo D 2018 Microstructure and mechanical properties of Fe-Cr-2Ni-Mo-V steel in carburizing process *Procedia Manufacturing* **15** 1612–8
[7] David D, Zdenek J, Zbynek S, Zdenek P and Emil S 2020 Quality evaluation of carburized surfaces of steels used in military technology *Manufacturing technology* **20** 2
[8] Farivar H, Deepu M J, Hans M, Phanikumar G, Bleck W and Prahl U 2019 Influence of post-carburizing heat treatment on the core microstructural evolution and the resulting mechanical properties in case-hardened steel components *Materials Science & Engineering A* **744** 778–89
[9] George K 2014 Microstructures and Properties of Carburized Steels *Heat Treating of Irons and Steels* 4D (United States: ASM International) (https://doi.org/10.31399/asm.hb.v04d.a0005982)
[10] Chengming L, Qi H, Weizhong T and Fanxiu L 2004 Carburising of steel AISI 1010 by using a cathode arc plasma process *Surface & Coatings Technology* **187** 1–5
[11] Yan M F and Liu Z R 2001 Study on microstructure and microhardness in surface layer of 20CrMnTi steel carburised at 880°C with and without RE *Mater. Chem. Phys.* **72** 97–100
[12] Scheuer C J, Cardoso R P, Mafra M and Brunatto S F 2013 AISI 420 martensitic stainless-steel low-temperature plasma assisted carburizing kinetics *Surf. Coat. Technol.* **214** 30–7
[13] Li F Z and Li C Z 1985 The influence of heat treatment after carburizing and retained austenite in the carburized layer on the strength and toughness of steel *Trans. Heat Treat. Met.* **6** 59–68
[14] Nart E and Genel K 2010 Investigation of carburising treatment of injector flange in diesel engine *Mater. Des.* **31** 2110–7
[15] Peifeng C, Yunkun L, Wenchao Y, Shaopeng Y, Fangzhong H, Jie S, Maoqiu W and Li L 2020 Comparison of very high cycle fatigue properties of 18CrNiMo7-6 steel after carburizing and pseudo-carburizing *J. Mater. Eng. Perform.* **29** 8340–7
[16] Yong T, Haojie W, Xiaoxue A and Zhaodong W 2019 Experimental study on carbon flux in vacuum carburizing *Mater. Res. Express* **6** 9
[17] Wei L, Aiwen L, Yilong L, Zhenglai Z and Jie C 2020 Effect of vacuum carburizing on surface properties and microstructure of a tungsten heavy alloy *Mater. Res. Express* **7** 016558
[18] Preston S 1991 Bending fatigue strength of carburising steel SS 2506 *Mater. Sci. Technol.* **7** 105–10
[19] Olga K and Richard D 2009 Effect of alloy composition on carburizing performance of steel *Journal of Phase Equilibria and Diffusion* **30** 235–41
[20] Wu C, Xiaofei H, Wenchao Y, Maoqiu W and Kefu Y 2021 Microstructure, hardness, and tensile properties of vacuum carburizing gear steel *Metals - Open Access Metallurgy Journal* **11** 300
[21] Heintzberger P J 2020 Influence of the temperature of vacuum carburizing on the thickness of the carburized layer and properties of steel parts *Met. Sci. Heat Treat.* **62** 37–43
[22] Grosch J 2014 Microstructure and properties of gas carburized steels *In Comprehensive Materials Processing* 1st ed. (Amsterdam, The Netherlands: Elsevier) pp 379–411
[23] Roy S and Sundararajan S 2016 The effect of heat treatment routes on the retained austenite and tribomechanical properties of carburized AISI 8620 steel *Surf. Coat. Technol.* **308** 236–43
[24] Pandey C, Giri A and Mahapatra M M 2016 Effect of normalizing temperature on microstructural stability and mechanical properties of creep strength enhanced ferritic P91 steel *Materials Science & Engineering A* **657** 173–84
[25] Colin P W, Ian H, Edmund J C and Duncan H G 2009 Facile synthesis of bimetallic carbonitrides, $V_{1-x}Ti_x$(C,N), by microwave carbothermal reduction–ammonolysis/carburisation (MW-CRAC) methods *J. Eur. Ceram. Soc.* **29** 2355–61
[26] Aissani L, Fellah M, Radjehi L, Nouveau C, Montagne A and Alhussein A 2019 Effect of annealing treatment on the microstructure, mechanical and tribological properties of chromium carbonitride coatings *Surf. Coat. Technol.* **359** 403–13
[27] Adams S M and Suleiman I Y 2018 Effect of carburization time and temperature on the mechanical properties of mild steel *Nigerian Research Journal of Engineering and Environmental Sciences* **3** 800–4
[28] Oyetunji A and Adeosun S O 2012 Effects of carburizing process variables on mechanical and chemical properties of carburized mild steel *Journal of Basic & Applied Sciences* **8** 319–24
[29] Eunji Y H J, Kun S K, Eui J K and Jongryoul K 2013 Influence of carbide formation on tensile and fatigue properties of carburized steels *Applied Microscopy* **43** 81–7
[30] Thibaux P, Méténier A and Xhoffer C 2007 Carbon diffusion measurement in austenite in the temperature range 500 °C to 900 °C *Metallurgical and Materials Transactions A* **38** 1169–76
[31] Giordani T, Clarke T R, Kwietniewski C E F, Aronov M A, Kobasko N I and Totten G E 2013 Mechanical and metallurgical evaluation of carburized, conventionally and intensively quenched steels *J. Mater. Eng. Perform.* **22** 2304–13
[32] Shima P, Hamid R K Z, Seyyed S G B and Mahesh C S 2019 Detection and estimation of retained austenite in a high strength Si-bearing bainite-martensite retained austenite micro-composite steel after quenching and bainitic holding (Q&B) *Metals* **9** 492
[33] Pavan H, Sathyashankara S, Gowrishankar M C, Manjunath S and Gurumurthy B M 2020 Effect of post carburizing treatments on residual stress distribution in plain carbon and alloy steels– a numerical analysis *Journal of Materials Research and Technology* **9** 8439–50

[34] Younes B 2018 Carburizing treatment of low alloy steels: Effect of technological parameters *J. Phys. Conf. Ser.* **1033** 012008
[35] Bin L, Bo W and Jianfeng G 2019 Effect of ammonia addition on microstructure and wear performance of carbonitrided high carbon bearing steel AISI 52100 *Surf. Coat. Technol.* **361** 112–8
[36] Guo-meng L, Yi-long L, Cun-hong Y, Hao S and Zhen-long Z 2019 Study of M50NiL steel under carburizing and nitriding duplex treatment *Surf. Coat. Technol.* **375** 132–42
[37] Rabah B, Omar A, Younes B and Zied D 2020 Effect of the carburizing layer on the morphology of chromium carbides *Journal of Siberian Federal University. Engineering & Technologies* **13** 187–93
[38] Hesham E 2014 Effect of carburization on the mechanical properties of the mild steel *International Journal of Innovation and Applied Studies* **6** 987–94